21

Non-Invasive Evaluation Method for Cartilage Tissue Regeneration Using Quantitative-MRI

Shogo Miyata
KEIO University
Japan

1. Introduction

Articular cartilage is an avascular tissue covering articulating surfaces of bones and it functions to bear loads and reduce friction in diarthrodial joints. The cartilage can be regarded as a porous gel, mainly composed of large proteoglycan (PG) aggregates having a negative fixed-charge density (nFCD), a water-swollen network of collagen fibrils, and interstitial water, all of which play important roles in load-bearing properties (Lee et al., 1981; Mow et al., 1980).

Although articular cartilage may function well over a lifetime, traumatic injury or the degenerative changes associated with osteoarthritis (OA) can significantly erode the articular layer, leading to joint pain and instability. Because of its avascular nature, articular cartilage has a very limited capacity to regenerate and repair. It is well-known that the natural response of articular cartilage to damage is variable and, at best, unsatisfactory.

Therefore, numerous studies have reported tissue-engineering approaches to restore degenerated cartilage and to repair defects; these approaches involve culturing autologous chondrocytes *in vitro* to create three-dimensional tissue that is subsequently implanted. In these tissue engineering approaches, it is important to assess the biomechanical and biochemical properties of the engineered cartilage. These material properties of the engineered constructs are detectable only via direct measurements that are invasive and require destructive treatments such as histological analysis, biochemical quantification, and mechanical testing. The application and utilization of these tissue-engineering approaches in a clinical setting requires a non-invasive method of evaluating biomechanical and biochemical properties of the actual regenerated cartilage for transplantation. Moreover, the method should be applicable to various aspects of cartilage regenerative medicine, including the characterization of the regenerated tissue during *in vitro* culture and *in vivo* evaluation after transplantation.

Magnetic resonance imaging (MRI) of articular cartilage is well accepted and has become common in recent years. Quantitative MRI techniques have been successfully developed to measure the macromolecular state within cartilage tissue. For example, the relationship between the water content of the degenerated cartilage and water self-diffusion has been

reported (Shapiro et al., 2001), while the transverse relaxation time T2 has been related to collagen concentration (Fragonas et al., 1998) and the spatial distribution of collagen, including both fibril orientation and organization (Nieminen et al., 2001; Xia et al., 2002).

The gadolinium-diethylene triamine pentaacetic acid (Gd-DTPA^{2-})-enhanced T1 imaging technique has been used to predict PG content (Bashir et al., 1996) and spatial distribution (Bashir et al., 1999). Furthermore, nFCD can be estimated from consecutive T1 relaxation time measurements using Gd-DTPA^{2-}-enhanced MRI and related to PG concentration. This MRI technique is already well-known as the "delayed Gadolinium Enhanced Magnetic Resonance Imaging of Cartilage" (dGEMRIC) technique. This technique is based on the utilization of the two-negative charge of the MRI contrast agent (i.e., Gd-DTPA^{2-}). Sulfated glycosaminoglycans (sGAG) in the PGs are negatively charged in the cartilage, giving rise to nFCD; the electric exclusion force between this nFCD and the negatively charged contrast agent result in the inverse distribution of the contrast agent to the PG distribution in the cartilage. Consequently, relaxation time (T1) and nFCD—as determined by dGEMRIC technique —correlate with PG concentration.

Previous studies have reported that, in tissue-engineered cartilage, MR measurements of regenerated cartilage showed correlations with biochemical properties (Potter et al., 2000) and biomechanical properties (Chen et al., 2003). Additionally, the sGAG content and the compressive modulus—the latter of which was determined by unconfined compression tests—showed a trend toward correlation with the nFCD, as determined by the Gd-DTPA^{2-}-enhanced MRI technique (Chen et al., 2003; Ramaswamy et al., 2008). In our earlier study, we reported that the nFCD of tissue-engineered cartilage determined by GD-DTPA^{2-}-enhanced MRI has been found to correlate with sGAG content (Miyata et al., 2006).

Although the non-invasive assessment of tissue integration and the non-destructive evaluation of molecular structure of the engineered cartilage are important, we believe no previous study has fully evaluated the relationships between the biomechanical properties and MRI measurements of regenerated cartilage consisting of articular chondrocytes. Previous study has indicated that MR images of autologous chondrocyte transplants may show clinically significant variations; neither biochemical properties nor the FCD of regenerated articular cartilage has been evaluated.

In this chapter, we introduce our evaluation technique for tissue-engineered cartilage using quantitative-MRI. We tested the hypothesis that MRI measurements of tissue-engineered cartilage correlate with biomechanical and biochemical properties and that these novel approaches can be used to evaluate cartilaginous matrix material properties during tissue regeneration.

2. Quantitative Magnetic Resonance Imaging (MRI) of tissue engineered cartilage

2.1 Isolation of chondrocytes and preparation of chondrocyte-seeded agarose constructs

We used agarose gel culture for tissue-engineered cartilage model, because agarose is a biocompatible, thermosensitive hydrogel that offers superior homogeneity and stability for

assessing both biomechanical and biochemical properties during *in vitro* culture, and has been used widely in cartilage mechanobiology. Chondrocyte-seeded agarose gels were prepared as described previously (Miyata et al., 2006; Miyata et al., 2004).

Articular chondrocytes were obtained from the glenohumeral joints of freshly slaughtered 4- to 6-week-old calves, from a local abattoir. Articular cartilage was excised from the humeral head, diced into ~1 mm^3 pieces, then shaken gently in Dulbecco's Modified Eagle's Medium/Ham's F12 (DMEM/F12) supplemented with 5% fetal bovine serum (FBS), 0.2% collagenase type II, and antibiotics-antimycotics, for 8–10 h at 37°C. Cells were then isolated from the digest by centrifugation and rinsed twice with phosphate buffered saline (PBS). Finally, after the isolated cells were resuspended with feed medium (DMEM/F12 supplemented with 20% FBS, 50 μg/mL L-ascorbic acid, and antibiotics-antimycotics), and the total number of cells was counted with a hemocytometer.

The isolated chondrocytes in the feed medium were mixed with an equal volume of PBS containing agarose with a low melting temperature (Agarose type VII, Sigma, MO) at 37°C, to prepare 1.5×10^7 cells/mL in 2% (wt/vol) agarose gel; it was then cast in a custom-made mold to make a large gel plate. After gelling at 4°C for 25 minutes, approximately 50 disks of 8-mm diameter, 1.5-mm thickness were cored out from the large gel plate with a biopsy punch. The chondrocyte-seeded agarose disks were fed 2.5 mL feed medium/disk, every other day and maintained in a 5% CO_2 atmosphere at 37°C.

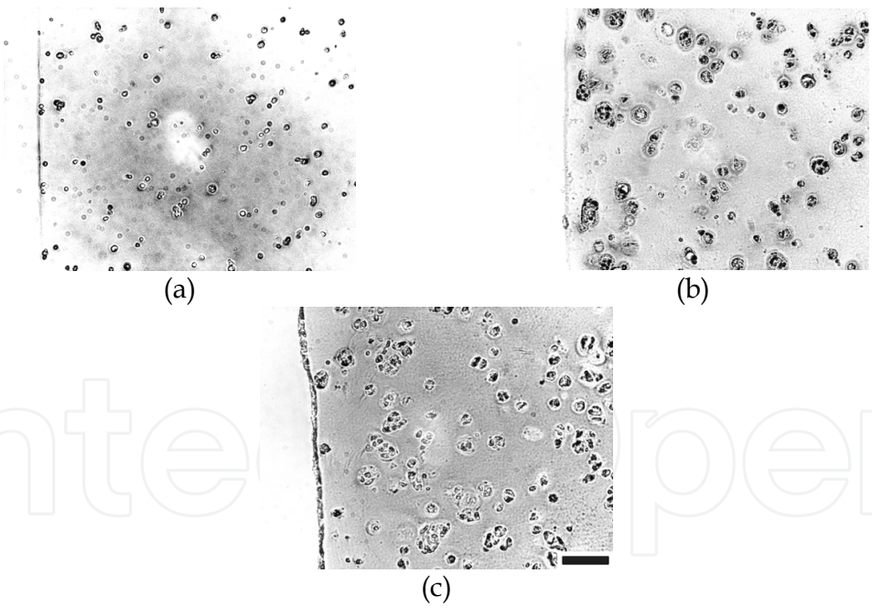

Fig. 1. Histological appearance of tissue-engineered cartilage at day 3 (a), day 10 (b), and day 28 (c), stained with alcian blue (Miyata et al., 2010). Scale bar = 100 μm.

Alcian blue-stained sections of the cultured specimens are shown in Fig. 1. Over the culture period, the chondrocytes in the agarose gel appeared rounded in shape, similar to those in the "native" articular cartilage. As shown in Fig. 1, the chondrocytes synthesized a thin shell of pericellular matrix (~day 10) and expanded the volume of the cartilaginous matrix (~day 28).

2.2 Magnetic Resonance Imaging (MRI) of cultured chondrocyte-seeded agarose gel

Quantitative MRI evaluations were performed on a 2.0-T Biospec 20/30 System with a B-GA20 Gradient System (Bruker, Karlsruhe, Germany) with a maximum gradient strength of 100 mT/m. The MRI data acquisition and reconstruction were performed using the ParaVision (Bruker) software system. In all MRI experiments, three or four sheets of the disks were stacked in layers and placed into glass tubes containing phosphate buffered saline (PBS) (Fig. 2). The measured parameters included longitudinal (T1) and transverse (T2) relaxation time and water self-diffusion coefficient (Diff). A longitudinal relaxation time map (T1-map) was obtained with a short echo time (TE: 15 ms) spin-echo sequence with different repetition time values (TR: 100 ms to 15 s, 16 steps). A transverse relaxation time map (T2-map) was obtained with a long repetition time value (TR: 15 s) spin-echo sequence with different echo time values (TE: 30 ms to 450 ms, 29 steps). A diffusion coefficient map (Diff-map) was calculated from the images obtained using a conventional diffusion weighted spin-echo (SE-DWI, TR: 15 s, TE: 35 ms) sequence with different b values (0, 74, 275, 603, 1059 s/mm^2). All sequences were performed with a field of view (FOV) of 50 × 50 mm^2, matrix size 64 × 64, and slice thickness 3 mm. The values of the relaxation time (T1 and T2) and the relative diffusion coefficient (Diff*) were calculated as the average of the specimen from the obtained T1-, T2-, and Diff-maps. The value of Diff* (= $Diff_S/Diff_P$) was calculated by normalizing the diffusion coefficient of the sample ($Diff_S$) by the diffusion coefficient of PBS ($Diff_P$) around the sample. All MRI measurements were carried out with no contrast agent at room temperature (23°C).

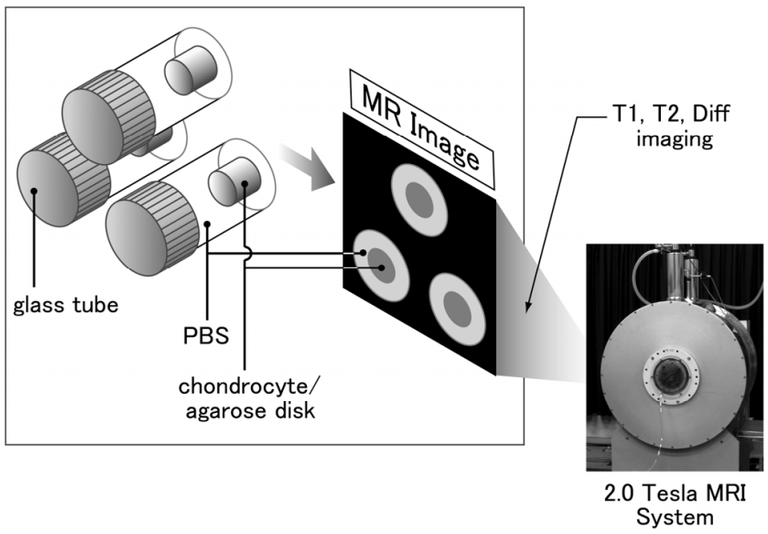

Fig. 2. Schematic diagram of MR Imaging (Miyata et al., 2007).

Figure 3−5 shows the MRI maps of the engineered cartilage. At the first stage of the culture (day 1), T1 and Diff of the engineered cartilage showed values similar to those of the PBS around the cartilage; hence, it was difficult to distinguish the boundaries between the engineered cartilage and the bath solution (PBS) in the MRI maps (Fig. 3a and 5a). By the end of the culture (day 28), the boundaries were distinguished in both T1- and Diff-maps (Fig. 3a−3c and 5a−5c). In contrast, the boundary between the specimen and the PBS remained clear in the T2-map during the culture time (Fig. 4a−4c). The T1, T2, and Diff

values of the engineered cartilage were averaged, and the results are summarized in Figure 6. T1 and Diff* of the tissue-engineered cartilage had decreased with an increase in the culture time (Fig. 6a and 6c). On the other hand, T2 of the engineered cartilage showed considerably lower values than those of the PBS in the glass tube throughout the culture time, and these values tended to increase slightly with the culture time (Fig. 6b).

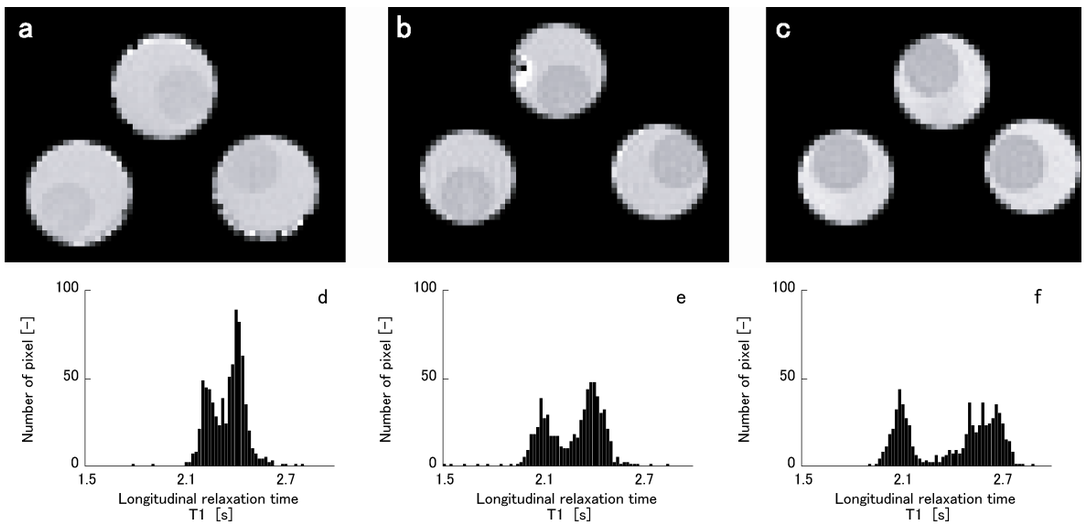

Fig. 3. T1-maps of day 1 (a), day 7 (b), and day 28 (c) post-inoculation specimens, and histograms of the T1 values derived from the MR images on day 1 (d), day 7 (e), and day 28 (f) (Miyata et al., 2007).

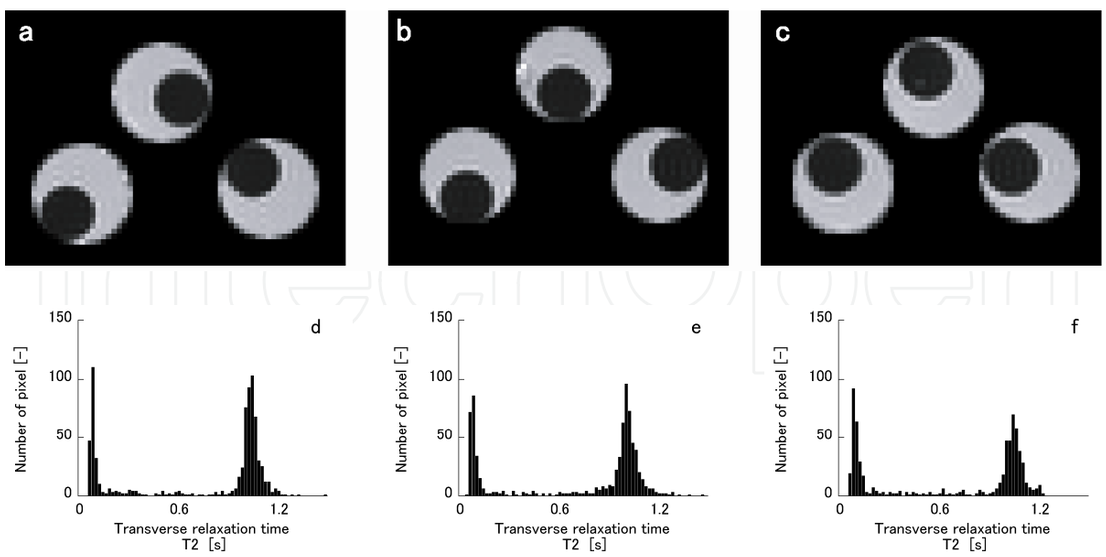

Fig. 4. T2-maps of day 1 (a), day 7 (b), and day 28 (c) post-inoculation specimens, and histograms of the T2 values derived from the MR images on day 1 (d), day 7 (e), and day 28 (f) (Miyata et al., 2007).

Consistent with the results of previous studies (Chen et al., 2003; Potter et al., 1998), our results showed that both T1 and Diff* decreased with an increase in the culture time. On the other hand, T2 tended to increase slightly by the end of the culture time. To understand the MRI properties of the tissue water protons, we have to understand the behavior of water molecules in the tissue at different stages of tissue maturity. With tissue growth and development, proteoglycan and collagen molecules accumulate in the agarose gel, resulting in a large fraction of macromolecule-associated water, which is known as "bound" water. Generally, the water molecules in the "bound" condition show short T1 and T2 relaxation times due to a reduced mobility as compared to "free" water. Thus, water proton relaxation curves, which were described by a single exponential, are derived from the weighted sum of the relaxation behavior of the "free" and "bound" water molecules in the engineered cartilage. This is consistent with our results that the T1 relaxation time and Diff* decreased with an increase in the content of cartilaginous matrix in the agarose gel. In the case of transverse relaxation, the T2 relaxation time of the engineered cartilage showed a value similar to that of the "native" articular cartilage (75–90 ms measured by our MRI system) from the early phase of the culture; further, T2 tended to increase slightly with tissue maturation. Based on this result, we speculate that the transverse relaxation of the water molecules in the engineered construct might be mainly affected by its association with the agarose molecules.

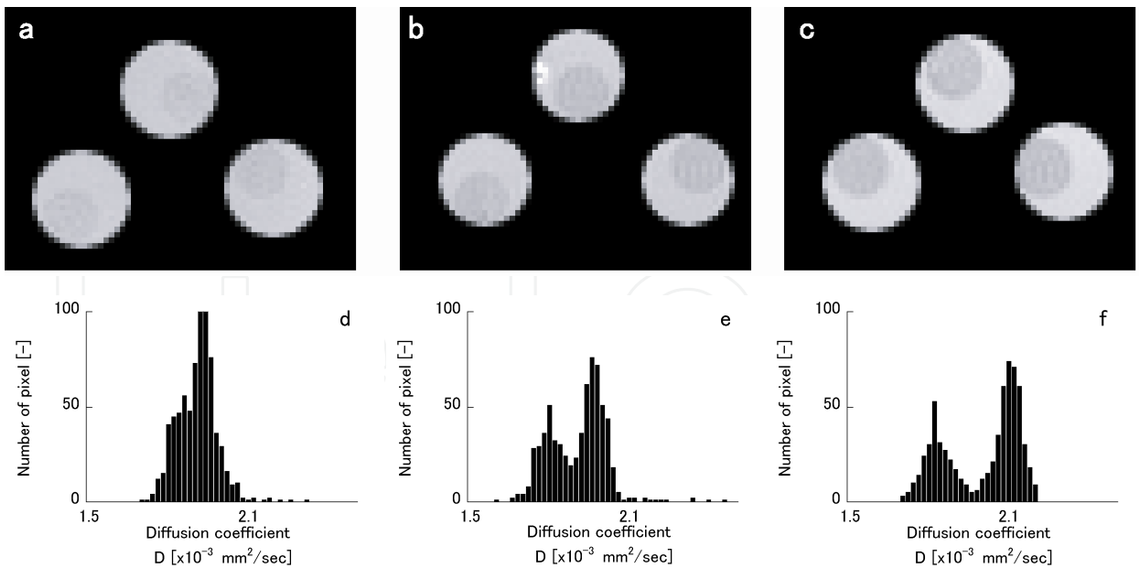

Fig. 5. Diff-maps of day 1 (a), day 7 (b), and day 28 (c) post-inoculation specimens, and histograms of the Diff values derived from the MR images on day 1 (d), day 7 (e), and day 28 (f) (Miyata et al., 2007).

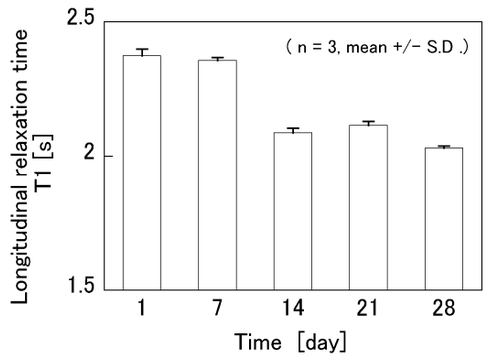

(a)

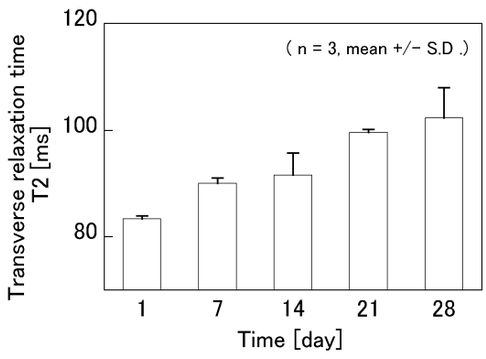

(b)

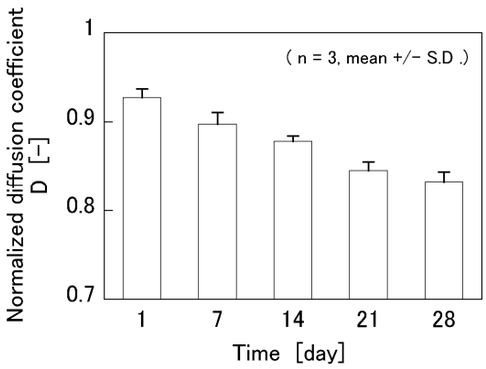

(c)

Fig. 6. Longitudinal relaxation time (a), transverse relaxation time (b), and relative diffusion coefficient (c) of the tissue-engineered cartilage during the culture time (Miyata et al., 2007). The values represent mean +/− S.D. (n = 3).

2.3 Evaluation of fixed charge density of tissue-engineered cartilage

For 'native' articular cartilage, the gadolinium-diethylene triamine pentaacetic acid (Gd-DTPA^{2-}) -enhanced T1 imaging technique has been used to predict the PG content (Bashir et

al., 1996) and spatial distribution (Bashir et al., 1999). Furthermore, the negative fixed charge density (nFCD) can be estimated from consecutive T1 relaxation time measurement using Gd-DTPA^{2-}-enhanced MRI and be related to the PG concentration. In this study, we used this dGEMRIC technique to monitor and evaluate tissue integration of the engineered cartilage.

The MRI measurements were performed with a 2.0-Tesla Bruker Biospec 20/30 system using Gd-DTPA^{2-} contrast agent. In all MRI measurements, the specimens were put into glass tubes filled with PBS (Fig. 7). The longitudinal relaxation time map, T1-map, was obtained with a short-echo time (TE: 15 ms), spin-echo sequence with different repetition time values (TR: 100 ms to 15 s, 16 steps). Subsequently, the specimens were balanced in PBS containing 1 mM Gd-DTPA^{2-} (Magnevist®, Nihon Schering, Osaka, Japan) for 10−12 hours; the longitudinal relaxation time map in the contrast agent, $T1_{Gd}$-map, was obtained again with a short-echo time (TE: 15 ms), spin-echo sequence with different repetition time values (TR: 30 ms to 5 s, 13 steps). Finally, using the relaxivity (R) value of Gd-DTPA^{2-} in saline (5.24 in our MRI system), the concentration of the contrast agent was estimated using the formula [Gd-DTPA^{2-}] = $1/R(1/T1_{Gd} - 1/T1)$. The negative fixed charge density (FCD) was calculated as follows

$$\mathrm{nFCD} = \frac{[\mathrm{Na}^+]_b\sqrt{[\mathrm{Gd-DTPA}^{2-}]_t}}{\sqrt{[\mathrm{Gd-DTPA}^{2-}]_b}} - \frac{[\mathrm{Na}^+]_b\sqrt{[\mathrm{Gd-DTPA}^{2-}]_b}}{\sqrt{[\mathrm{Gd-DTPA}^{2-}]_t}} \tag{1}$$

where subscript *b* stands for bath solution and subscript *t* stands for cartilaginous tissue(Bashir et al., 1996). All MRI measurements were performed at room temperature 23°C.

In the gadolinium-enhanced MR imaging measurements, longitudinal relaxation time of the bulk PBS containing Gd-DTPA reagent showed 0.179 ± 0.06 seconds in our MRI system. The $T1_{Gd}$ of the cultured specimen increased as a function of tissue maturation (0.197 ± 0.001 to 0.222 ± 0.003 seconds). At the first stage of the culture (day 3), $T1_{Gd}$ of the tissue-engineered cartilage showed values proximate to those of the PBS containing the Gd-DTPA^{2-} agent around the engineered cartilage; hence, it was difficult to distinguish the boundaries between the engineered cartilage and the bath solution in the $T1_{Gd}$-maps (Fig. 8a). By the end of the culture (day 28), the boundaries had become distinct in the T1Gd-maps (Fig. 8). The [Gd-DTPA^{2-}] in the engineered cartilage decreased with increases in culture time. The nFCD, as determined from the [Gd-DTPA^{2-}] in the specimen and bath solution, increased with culture time (Fig. 9).

As time in culture lengthened, the gross appearance of the cultured disk became increasingly opaque. The DMMB assay (Farndale et al., 1986) revealed that the sGAG content of the chondrocyte/agarose disks increased as a function of tissue maturation (0.19 ± 0.27 to 13.2 ± 1.9 mg/mL-disk-vol). Finally, the sGAG content of the reconstructed cartilaginous disk reached approximately 20% of the "native" articular cartilage (data not shown).

To correlate gadolinium-enhanced MRI and biochemical properties, the sGAG content of the tissue was plotted as a function of the FCD. From the linear regression analysis, the FCD correlated significantly with the sGAG content ($r = 0.95$, $n = 30$, $P < 0.001$) (Fig. 10), and the tissue [Gd-DTPA^{2-}] correlated with the sGAG content by $r = 0.83$, $n = 30$, $P < 0.001$.

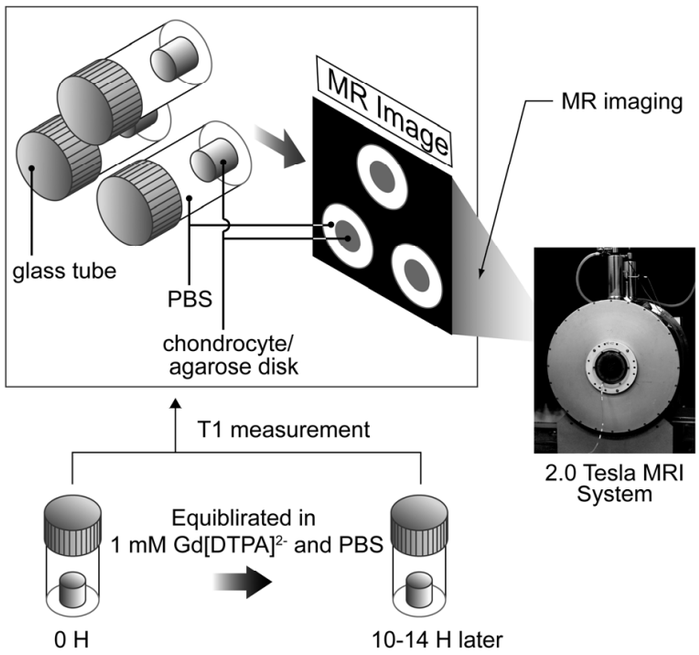

Fig. 7. Schematic diagram of gadolinium-enhanced MRI. In all MRI measurements, the cultured specimens were put into glass tubes filled with phosphate buffered saline (PBS) or 1 mM Gd DTPA^{2-} (Miyata et al., 2010).

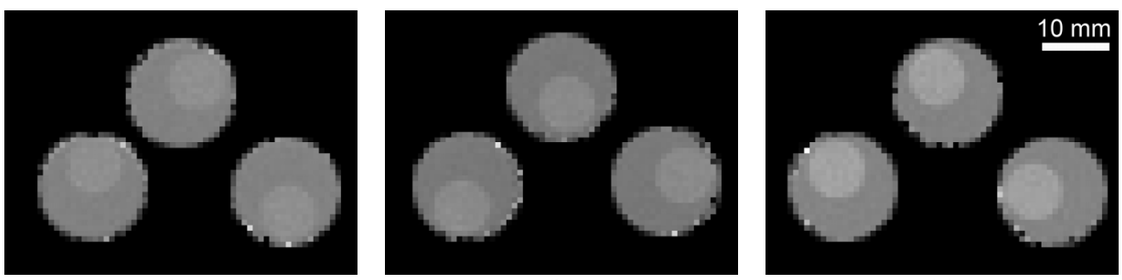

Fig. 8. Quantitative water proton T1 maps in the presence of Gd-DTPA2– at day 3 (a), day 7 (b), and day 28 (c) (Miyata et al., 2010).

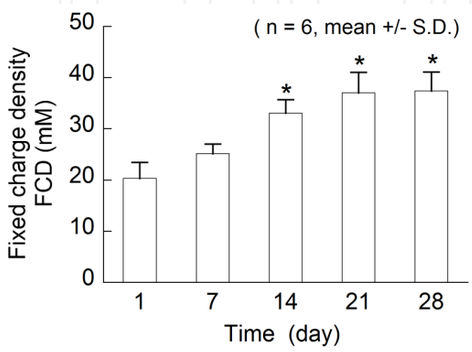

Fig. 9. Tissue fixed-charge density, with time in culture, for tissue-engineered cartilage (Miyata et al., 2010). * indicates significant difference from day 0 ($P < 0.05$).

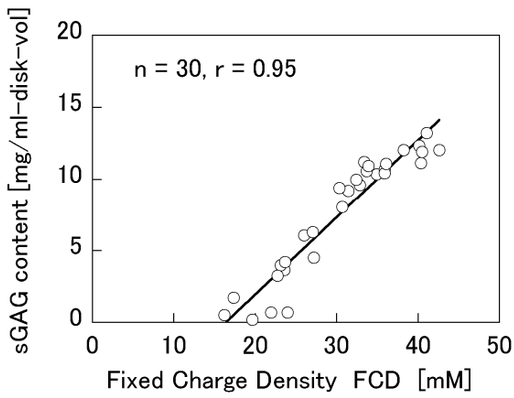

Fig. 10. Scatter plots relating the tissue fixed charge density (FCD) to the sulfated glycosaminoglycan (sGAG) content (Miyata et al., 2006).

2.4 Static and dynamic biomechanical testing of cultured agarose/chondrocyte constructs

Mechanical testing of the disk-shaped specimens was performed with unconfined compression, using impermeable stainless platens in PBS at room temperature. Static compressive properties were measured in a custom-made chamber attached to a material testing device (Autograph 5kNG, Shimadzu, Kyoto, Japan). Stress relaxation tests were performed by applying a ramp displacement at 0.05 mm/min to a 20% static compressive strain, followed by relaxation to equilibrium (2,400 s). The equilibrium compressive modulus (E_{eq}) was calculated from the imposed compressive strain and the equilibrium load, divided by the cross-sectional area of the specimen.

Dynamic compression tests were carried out using a viscoelastic spectrometer (DDV-MF, A&D, Tokyo, Japan) (Miyata et al., 2005). For preconditioning, a 20% static compressive strain was loaded and a sinusoidal displacement of 0.5% compressive strain was then superimposed at a frequency of 1 Hz. After equilibrium had been reached (approximately 20 min), a sinusoidal displacement of 0.5% compressive strain was applied at frequencies ranging from 0.01 to 5.0 Hz. The dynamic compressive modulus (E_{dyn}) was calculated from the ratio of the measured stress amplitude and the applied strain amplitude.

Figure 11 shows the means and standard deviations of the equilibrium compressive modulus E_{eq} and dynamic compressive modulus E_{dyn} versus time in culture, for the tissue-engineered cartilage. With respect to the static compressive property, significant differences were observed in the equilibrium compressive modulus. With increases in culture time, the E_{eq} of the specimens increased and reached approximately 10% of that of "native" cartilage from which the chondrocytes were harvested (0.45 ± 0.12 MPa, n =3). With respect to the dynamic compressive property, significant differences were also observed for testing conditions. The dynamic compressive modulus E_{dyn} of the engineered cartilage depended on both testing frequency and culture time. For each time point, E_{dyn} increased nonlinearly with increases in frequency. The engineered cartilage also exhibited marked stiffening with time in culture. The value of E_{dyn} increased with culture time at each testing frequency (0.01–2.0 Hz).

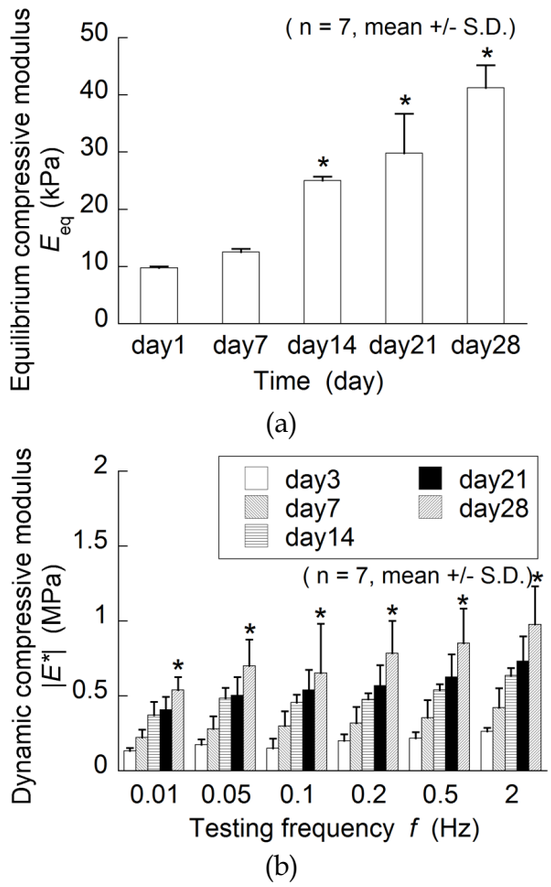

Fig. 11. Equilibrium compressive modulus E_{eq} (a) and dynamic compressive modulus E_{dyn} (b), with time in culture, for the cultured chondrocyte/agarose disks (Miyata et al., 2010). * indicates significant difference from day 0 ($P < 0.05$).

2.5 Relationships between MRI measurements and biomechanical properties of cultured chondrocyte-seeded constructs

To determine the correlations between the quantitative MRI measurements and the biomechanical and biochemical properties of the tissue-engineered cartilage, we performed linear regression analyses among the MRI-derived parameters (T1, T2, Diff, and FCD), the biochemical composition (sGAG content), and the biomechanical properties (E_{eq}, E_{dyn}) of the engineered cartilage.

To confirm the correlation, the E_{eq} of the engineered cartilage were plotted as functions of the T1, T2, and Diff, respectively. The E_{eq} of the engineered cartilage (Fig. 12a) showed a strong correlation with T1 and Diff but a weak correlation with T2 (Fig. 12b and 12c). Similarly, the tissue sGAG concentration (Fig. 13a and 13c) and were found to be strongly correlated with T1 and Diff. Consistent with the results of the previous investigation (Potter et al., 2000), our results showed that T1 relaxation time and Diff showed a significant correlation with the biomechanical properties and the sGAG content of the tissue-engineered cartilage. The results of recent studies have shown that the articular cartilage

degeneration induced by collagenase treatment resulted in changes in T2 relaxation time and the equilibrium modulus (Nieminen et al., 2000). In the present study, slight increase in T2 values was observed during the culture.

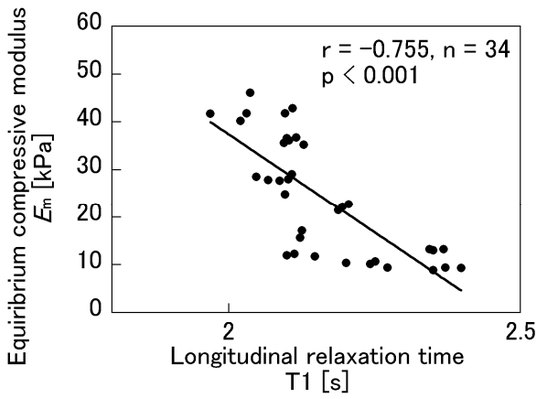

(a)

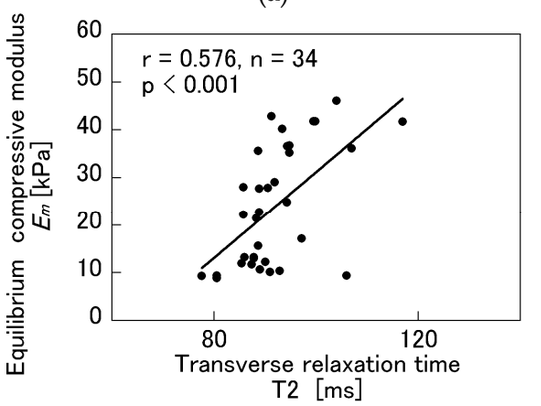

(b)

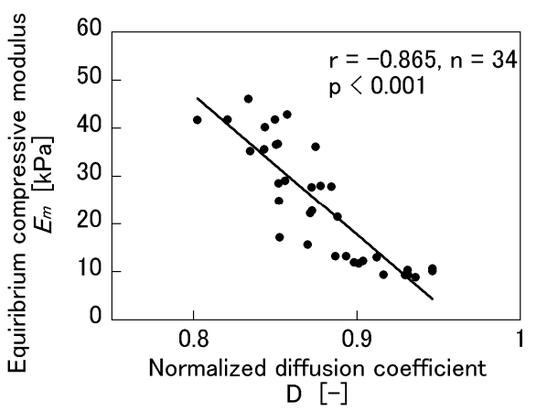

(c)

Fig. 12. Scatter plots for the relationship between the equilibrium compressive modulus E_{eq} and longitudinal relaxation time (a), transverse relaxation time (b), and relative diffusion coefficient (c) (Miyata et al., 2007). Solid line represents the linear regression line.

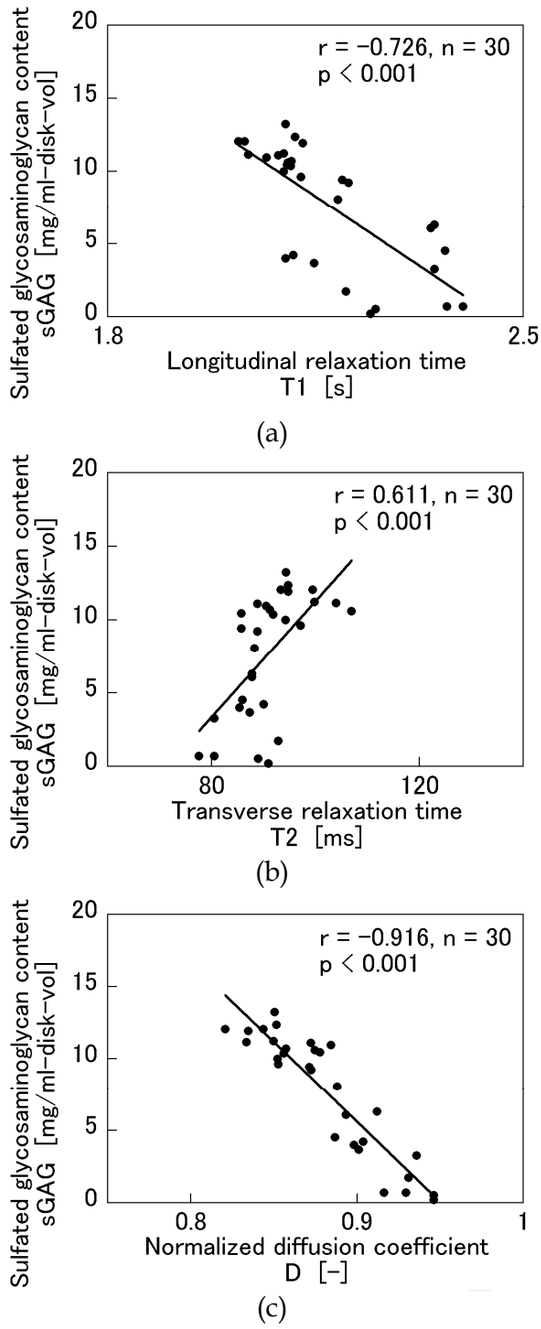

Fig. 13. Scatter plots for the relationship between the equilibrium compressive modulus E_{eq} and longitudinal relaxation time (a), transverse relaxation time (b), and relative diffusion coefficient (c) (Miyata et al., 2007). Solid line represents the linear regression line.

One possible explanation is that the changes in the biophysical properties might be mainly due to the altered sGAG content, and the synthesis of collagen and the reorganization of collagen network might be insufficient in the agarose gel culture.

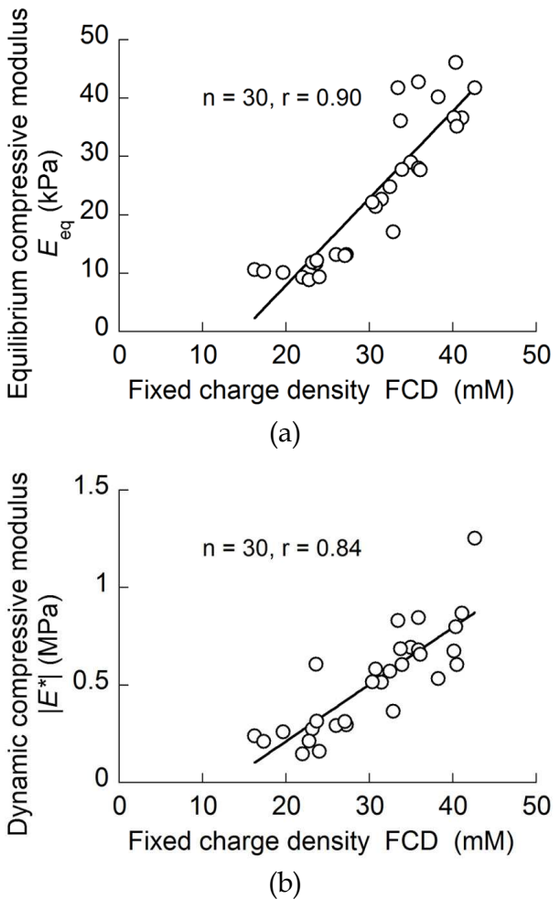

Fig. 14. Typical scatter plots relating the tissue fixed-charge density to equilibrium compressive modulus E_{eq} (a) and dynamic compressive modulus E_{dyn} at 0.5 Hz (b) (Miyata et al., 2010).

	R^2	P
FCD vs. E_{eq}	0.81	< 0.001
FCD vs. E_{dyn}, 0.01 Hz	0.79	< 0.001
FCD vs. E_{dyn}, 0.02 Hz	0.73	< 0.001
FCD vs. E_{dyn}, 0.05 Hz	0.73	< 0.001
FCD vs. E_{dyn}, 0.5 Hz	0.70	< 0.001
FCD vs. E_{dyn}, 2.0 Hz	0.71	< 0.001

Table 1. Linear Pearson correlations between biomechanical and Gd-DTPA^{2-}-enhanced MRI parameters in tissue-engineered cartilage (Miyata et al., 2010).

To evaluate the relationship between Gd-DTPA^{2-}-enhanced MRI parameters and biomechanical properties, the E_{eq} and E_{dyn} of the engineered cartilage were plotted as functions of the nFCD, respectively. From the linear Pearson correlation analysis, it was found that nFCD correlated significantly with E_{eq} and E_{dyn} (Table 1, Fig. 14). The equilibrium compressive modulus showed a higher correlation than the dynamic compressive modulus of all testing frequencies, and the dynamic compressive modulus tended to show a slightly higher correlation at low frequencies (0.01–0.05 Hz). The sGAG of articular cartilage plays a

crucial role in static compressive behavior, while collagen bears a dynamic compressive load (Korhonen et al., 2003). Therefore, the nFCD—which is to say, the sGAG content—might show a higher correlation with the equilibrium modulus than with the dynamic modulus. Moreover, the dynamic modulus showed a trend toward correlation with the nFCD at lower frequencies than that of higher frequencies. That might reflect the collagen network levels regenerated in the agarose gel. Nonetheless, the results of recent studies have shown that variations in collagen architecture among varieties of articular cartilage decreased the significance of correlations between Gd-DTPA^{2-}-enhanced MRI and mechanical properties, because the architecture of the collagen network, as well as PGs, plays an important role in the mechanicalproperties of articular cartilage (Nissi et al., 2007). In the present study, the chondrocytes in agarose gel reconstructed the immature collagen network, prompting a low-level effect on the compressive property compared to "native" articular cartilage; therefore, significant correlations might be found between Gd-DTPA^{2-}-enhanced MRI and compressive properties. From these facts, our evaluation methods using Gd-DTPA^{2-}-enhanced MRI could be applicable at the earlier stage of tissue regeneration.

3. Conclusion

In conclusion, we evaluated the changes in the quantitative MRI parameters and matrix FCD of tissue-engineered cartilage that consisted of articular chondrocytes and hydrogels. We found significant linear correlations between the quantitative MRI measurements and the biomechanical and biochemical properties of the engineered cartilage. Finally, we suggest that the quantitative MRI technique can be a useful, non-invasive approach to evaluate the biomechanical properties of regenerated cartilage during *in vitro* culturing process.

4. Acknowledgment

This research was supported in part by a Grant-in-Aid for Young Scientists (B) (No. 18700414) from the Ministry of Education, Science, Sports and Culture of Japan.

5. References

Bashir, A.; Gray, M. L. & Burstein, D. (1996). Gd-DTPA^{2-} as a Measure of Cartilage Degradation. *Magnetic Resonance Medicine*, Vol.36, pp.665-673

Bashir, A.; Gray, M.L.; Hartke, J. & Burstein, D. (1999). Nondestructive Imaging of Human Cartilage Glycosaminoglycan Concentration by MRI. *Magnetic Resonance in Medicine*, Vol.41, pp.857–865

Chen, C. T.; Fishbein, K.W.; Torzilli, P. A.; Hilger, A.; Spencer, R. G. & Horton, W. E., Jr. (2003). Matrix Fixed-Charge Density as Determined by Magnetic Resonance Microscopy of Bioreactor-Derived Hyaline Cartilage Correlates with Biochemical and Biomechanical Properties. *Arthritis and Rheumatism*, Vol.48, pp.1047-1056

Farndale, R. W.; Buttle, D. J. & Barrett, A. J. (1986). Improved Quantitation and Discrimination of Sulphated Glycosaminoglycans by Use of Dimethylmethylene Blue. *Biochimica et Biophysica Acta*, Vol.883, pp.173-177

Fragonas, E.; Mlynárik, V.; Jellús, V.; Micali, F.; Piras, A.; Toffanin, R.; Rizzo, R. & Vittur, F. (1998). Correlation between Biochemical Composition and Magnetic Resonance Appearance of Articular Cartilage. *Osteoarthritis and Cartilage*, Vol.6, pp.24–32

Korhonen, R.K.; Laasanen, M.S.; Töyräs, J.; Lappalainen, R.; Helminen, H.J. & Jurvelin, J.S. (2003). Fibril Reinforced Poroelastic Model Predicts Specifically Mechanical

Behavior of Normal, Proteoglycan Depleted and Collagen Degraded Articular Cartilage. *Journal of Biomechanics*, Vol.36, pp.1373–1379

Lee, R. C.; Frank, E. H.; Grodzinsky, A. J. & Roylance, D. K. (1981). Oscillatory Compressional Behavior of Articular Cartilage and Its Associated Electromechanical Properties. *Journal of Biomechanical Engineering*, Vol.103, pp. 280-292

Miyata, S.; Tateishi, T.; Furukawa, K. & Ushida, T. (2005). Influence of Structure and Composition on Dynamic Visco-Elastic Property of Cartilaginous Tissue: Criteria for Classification between Hyaline Cartilage and Fibrocartilage Based on Mechanical Function. *JSME International Journal: C*, Vol.48, pp.547–554

Miyata, S.; Homma, H.; Numano, T.; Furukawa, K; Tateishi, T. & Ushida, T. (2006). Assessment of Fixed Charge Density in Regenerated Cartilage by Gd-DTPA - Enhanced MR Imaging. *Magnetic Resonance and Medical Science*, Vol.5, No.2, pp. 73-78

Miyata, S.; Numano, T.; Homma, H.; Tateishi, T. & Ushida, T. (2007). Feasibility of Noninvasive Evaluation of Biophysical Properties of Tissue-Engineered Cartilage by Using Quantitative MRI. *Journal of Biomechnaics*, Vol.40, pp. 2990-2998

Miyata, S.; Homma, H.; Numano, T.; Tateishi, T. & Ushida, T. (2010). Evaluation of Negative Fixed-charge Density in Tissue-Engineered Cartilage by Quantitative MRI and Relationship with Biomechanical Properties. *Jounal of Biomechanical Engineering*, Vol.132, No.7, pp.071014

Mow, V.C.; Kuei, S. C.; Lai, W.M. & Armstrong, C.G. (1980). Biphasic Creep and Stress Relaxation of Articular Cartilage in Compression? Theory and Experiments. *Journal of Biomechanical Engineering*, Vol.102, pp.73-84

Nieminen, M.T.; Rieppo, J.; Toyras, J.; Hakumaki, J.M.; Silvennoinen, J.; Hyttinen, M.M.; Helminen, H.J. & Jurvelin, J.S. (2001). T2 Relaxation Reveals Spatial Collagen Architecture in Articular Cartilage: a Comparative Quantitative MRI and Polarized Light Microscopic Study. *Magnetic Resonance in Medicine*, Vol.46, pp.487-493

Nieminen, M.T.; Toyras, J.; Rieppo, J.; Hakumaki, J.M.; Silvennoinen, J.; Helminen, H.J. & Jurvelin, J.S. (2000). Quantitative MR Microscopy of Enzymatically Degraded Articular Cartilage. *Magnetic Resonance in Medicine*, Vol.43, pp.676-681.

Nissi, M.J.; Rieppo, J.; Töyräs, J.; Laasanen, M.S.; Kiviranta, I.; Nieminen, M.T. & Jurvelin, J.S. (2007). Estimation of Mechanical Properties of Articular Cartilage with MRI—dGEMRIC, T2 and T1 Imaging in Different Species with Variable Stages of Maturation. *Osteoarthritis and Cartilage*, Vol.15, pp.24–32

Potter, K.; Butler, J.J.; Adams, C.; Fishbein, K.W.; McFarland, E.W.; Horton, W.E. & Spencer, R.G. (1998). Cartilage Formation in a Hollow Fiber Bioreactor Studied by Proton Magnetic Resonance Microscopy. *Matrix Biology*, Vol.17, pp.513-523

Potter, K.; Butler, J.J.; Horton, W.E. & Spencer, R.G. (2000). Response of Engineered Cartilage Tissue to Biochemical Agents as Studied by Proton Magnetic Resonance Microscopy. *Arthritis and Rheumatism*, Vol.43, pp.1580-1590

Ramaswamy, S.; Uluer, M.C.; Leen, S.; Bajaj, P.; Fishbein, K.W. & Spencer, R.G. (2008). Noninvasive Assessment of Glycosaminoglycan Production in Injectable Tissue-Engineered Cartilage Constructs Using Magnetic Resonance Imaging. *Tissue Engineering Part C: Methods*, Vol.14, pp.243–249

Shapiro, E.M.; Borthakur, A.; Kaufman, J.H.; Leigh, J.S. & Reddy, R. (2001). Water Distribution Patterns Inside Bovine Articular Cartilage as Visualized by 1H Magnetic Resonance Imaging. *Osteoarthritis Cartilage*, Vol.9, pp.533-538

Xia, Y.; Moody, J.B. & Alhadlaq, H. (2002). Orientational Dependence of T2 Relaxation in Articular Cartilage: A Microscopic MRI (microMRI) Study. *Magnetic Resonance in Medicine*, Vol.48, pp.460–469

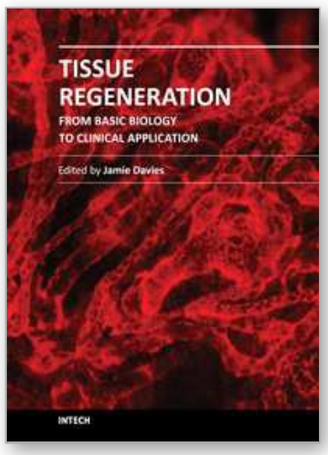

Tissue Regeneration - From Basic Biology to Clinical Application
Edited by Prof. Jamie Davies

ISBN 978-953-51-0387-5
Hard cover, 512 pages
Publisher InTech
Published online 30, March, 2012
Published in print edition March, 2012

When most types of human tissue are damaged, they repair themselves by forming a scar - a mechanically strong 'patch' that restores structural integrity to the tissue without restoring physiological function. Much better, for a patient, would be like-for-like replacement of damaged tissue with something functionally equivalent: there is currently an intense international research effort focused on this goal. This timely book addresses key topics in tissue regeneration in a sequence of linked chapters, each written by world experts; understanding normal healing; sources of, and methods of using, stem cells; construction and use of scaffolds; and modelling and assessment of regeneration. The book is intended for an audience consisting of advanced students, and research and medical professionals.

INTECH
open science | open minds

InTech Europe
University Campus STeP Ri
Slavka Krautzeka 83/A
51000 Rijeka, Croatia
Phone: +385 (51) 770 447
Fax: +385 (51) 686 166
www.intechopen.com

InTech China
Unit 405, Office Block, Hotel Equatorial Shanghai
No.65, Yan An Road (West), Shanghai, 200040, China
中国上海市延安西路65号上海国际贵都大饭店办公楼405单元
Phone: +86-21-62489820
Fax: +86-21-62489821

IntechOpen